

Distribution Network Performance Enhancement Through Optimal Sizing and Placement of D-STATCOM using Particle Swarm Optimization Technique (case study-Woldya Distribution Network)

ESUBALEW FIKRU GETAHUN, ASEFA SISAY YIMER*, WONDWOSSEN ASTATIKE HAILE

Electrical and Computer Engineering Department,
Kombolcha Institute of Technology, Wollo University
KOMBOLCHA, ETHIOPIA.

*Corresponding Author

Abstract: This article presents the use of distribution static synchronous compensator (D-STATCOM) to improve distribution network performance by maintaining voltage profile, stability and reducing power losses. The study was conducted on a 7.2 MW Gonder ber feeder, which had an unacceptable voltage profile and high active and reactive power losses. Two methods were applied to assign the power control variables: bus-based voltage stability index analysis and particle swarm optimization (PSO). The optimal allocation was tested in different system cases. The results showed that a single installation of D-STATCOM improved system performance; with an improved voltage profile between 0.95 and 1.05p.u, increased voltage stability indices and reduced active and reactive power losses. Cost analysis of the proposed compensation scheme indicated a payback period of 1.8 years.

Keywords: D-STATCOM, power loss, voltage profile, PSO, voltage stability index, MATLAB Software.

Received: April 21, 2024. Revised: October 11, 2024. Accepted: November 13, 2024. Published: December 10, 2024.

1 Introduction

Today, the main problem is to balance the energy demand with the voltage magnitude while minimizing power losses. Distribution systems must provide diverse customers with varied demand patterns. Inductive loads cause significant power losses in long radial networks, operating close to voltage instability limits. This causes network overload, increased power losses, reduced voltage profile and associated problems. The energy generated leads to high losses in transmission and distribution. Based on several studies carried out around the world, the amount of losses on the distribution side is estimated at 13% of the total energy produced [1]. Proper compensation methods are essential to maintain the voltage profile in distribution systems. Two commonly used techniques are series voltage regulators and shunt capacitors. Series regulators step down voltage, generate reactive power, and have a slow response. Shunt capacitors have limitations in terms of continuously variable reactive power and natural oscillatory behavior [2].

2 Related works

Different researchers have proposed several ways to solve the problem of voltage drop, power loss and voltage instability in distribution systems. Some of them are reviewed as follows: Khan, BaseemRedae, Kalay Gidey, Esayas Mahela, PrakashTaha, Ibrahim B.M.Hussien, Mohammed G uses the Improved Bacterial Foraging Algorithm (IBFA) to optimize the sizing and

placement of DSTATCOM in the distribution subdivision, minimizing the power losses and improving stability and voltage profile.[3]. E. Ijmtst demonstrates the use of a back-propagation control algorithm to perform a three-stage delivery static compensator (DSTATCOM), including load balancing and zero-voltage management of reactive power compensation under nonlinear loads [4]. IM Mehedi et al., Mehédi et al. propose a FACTS-based method to minimize fault current in systems, improve the performance of switchgear and protection equipment, and enable higher power transmission via static synchronous series compensators and power flow controllers unified [5]. AA Abou El-Ela, RA El-Sehie my, AM Kinawy and MT Mouwafi, This study proposes a two-step procedure for identifying optimal locations and sizes of capacitors in radial distribution systems. It uses loss sensitivity analysis and an ant colony optimization algorithm, taking into account energy losses and capacitor costs. The study also considers fixed and practical switches and capacitor combinations [6]. OE Olabode, IK Okakwu, AS Alayande and TO Ajewole, the paper presents a two-step approach to sizing shunt capacitors and identifying their Optimal placement in radial distribution systems. It uses a multi-objective function to minimize power losses and improve the bus voltage profile, a weighted approach and the Cuckoo search algorithm for load flow analysis [7]. Search algorithm. G. Niazi and M. Lalwani This paper discusses the research and development of particle swarm optimization (PSO) algorithm for distributed generation optimal placement (ODGP) problems, reviewing various

models and methods [8]. Wondossen. A. and P. Chandrasekar, this article deals with the study of design and analysis of micro grids in a rural village using HOMER Pro software. The hybrid system, consisting of wind turbines, diesel and solar panels, aims to provide reliable and cost-effective electrical energy [9]. Chitransh Shrivastava, Manoj Gupta, Dr. Atul Koshti PG This paper presents an approach based on a forward-backward scanning method for load flow analysis in a radial distribution system to improve voltage stability and minimize losses on transmission lines, taking into account takes into account the cost function for planning the entire power system, and has been tested on the IEEE-33 standard. bus system tested on IEEE-33 bus system [10]. Moufid, Ismail El Markhi, Hassane El Moussaoui, Hassan Tijani and Lamhamdi This article discusses the use of a synchronous static compensator (STATCOM) to improve the voltage in the IEEE 14 bus power system network. The study analyzes the system using standard test data and STATCOM, by comparing the results with the original power flow to determine the optimal STATCOM location for improved voltage profiles [11]. Yuvaraj, T.Ravi, K. Devalalaji, K. R, This study uses curve fitting technique to optimize placement and sizing of DSTATCOM, thereby helping distribution network operators select size based on load changes on IEEE 33 and 69 bus radial distribution systems. Literature on optimal allocation methods has limitations, including single objective functions, long simulation times, and theoretical assumptions. This research aims to fill these gaps by focusing on optimal D-STATCOM placement and sizing, multi-objective optimization, fast convergence characteristics, economic preferences and system constraints for PSO simulation [12]

3 Problem formulation

3.1 Minimize active power losses

Active power losses in the distribution system should be minimized as much as possible for reliable power transfer. The total line losses in the distribution system can be calculated as follows:

$$F_1 = \sum_{i=1}^{NBr} R_i * I_i^2 \quad (1)$$

Where F_1 is the first term of the objective function associated with the system losses, I_i is the current of line i , R_i is the resistance of the i th line and NBr is the number of branches of the system [13].

3.2 Minimize bus voltage deviations

It is important to keep the bus voltage within the limit and the deviation from the rated voltage can be the second objective function. The objective function to improve the voltage profile is

$$F_2 = \sum_{i=1}^{Nbus} (V - V_i)^2 \quad (2)$$

Where F_2 is the second term of the objective function, V_i is the bus voltage and V is the reference voltage which is 1 pu [14].

3.3 Improved voltage stability

There are many indices used to check the safety level of the electrical system. In this section, a new steady-state voltage stability index is used to identify the node that has the highest risk of voltage collapse. The voltage stability index at each node is calculated using equation 3. The node which has the low value of VSI is the weakest node and the voltage collapse phenomenon will start from this node. The VSI is calculated from the load flow for all buses in the given system and the values are ranked in descending order. Therefore, to avoid the possibilities of voltage collapse, the VSI of the nodes must be maximized [15].

3.4 Choosing weighting values

This research study focuses on effectively reducing power losses in multi-objective functions to reduce total operating costs. The weights are assumed to be positive and limited to 0.5-0.8, 0.1-0.4 and 0.1-0.4, respectively. The real power loss reduction index is given more emphasis, while all three indices are taken into account. The condition $W_1 + W_2 + W_3 = 1$ must be satisfied in each case [16].

3.5 System constraints

From the results presented in Table 1 above, the weight combination chosen is the one that gives the best minimum physical condition. Thus, the weights chosen. $W_1 = 0.8$ for power loss reduction, $W_2 = 0.1$ for voltage profile improvement and $W_3 = 0.1$ for voltage stability index and the MOF was given by eqn.(3) [13]:

$$F = 0.8 * F_1 + 0.1 * F_2 + 0.1 * \frac{1}{F_3} \quad (3)$$

3.5.1 Voltage deviation limit

System voltage in all buses must be within an acceptable range

$$V_m^{\min} \leq |V_m| \leq V_m^{\max} \quad (4)$$

The system voltage is limited to $0.95pu \leq V_m \leq 1.05 Pu$ [13].

3.5.2 Reactive power compensation

The reactive power injected by D-STATCOM to the system is limited by a lower and upper limit as shown below.

$$Q_m^{\min} \leq |Q_m| \leq Q_m^{\max} \quad (5)$$

The reactive power injected by D-STATCOM is limited by 100KVar $\leq Q_m \leq 1250\text{KVar}$ [17].

3.5.3 Thermal limit

The energy flow crossing the lines is limited by the thermal capacity of the lines:

$$|S_{ij\min} \leq S_{ij\max}| \quad (6)$$

The power flow through the lines is limited with $S_{ij\max} = 100\text{MVA}$ [17].

4 Load flow analysis of radial distribution systems

For a given set of load conditions, load flow analysis of power networks is important to acquire data on voltage, active and reactive power of the system. It is a beneficial analysis, investigation of problems and optimal utilization of the distribution system. Newton Raphson, Gauss Seidel and decoupled load flow analysis are the most conventional and widely applicable methods in distribution and transportation systems. Nowadays, due to the radial nature of power lines, unbalanced loading, high R/X ratio, large number of buses, wide impedance range, problems convergence and related problems, conventional methods of load flow analysis become unsuitable for distribution systems. Following this forward/backward scanning charge flow analysis using Kirchhoff's laws, it becomes more suitable for distribution systems and was used in this work [18].

4.1 Forward/Backward Sweep Load flow method

This method uses forward and backward scanning processes to calculate node voltages and branch current in radial network topologies. It forms two derivative matrices called bus injection matrix to branch current (BIBC) and branch current to bus voltage matrix (BCBV) using Kirchhoff's current law and Kirchhoff's voltage law. The BIBC matrix can be expressed as a complex power absorbed by the load [18].

$$S_{Li} = P_{Li} + jQ_{Li} \quad (7)$$

Or $i = 1 \dots N$

Step 1: The backward sweeping branch currents are grouped from the charges to the origin for each iteration k. To find the branch current, the current injected on each bus and the bus injection to the branch current (BIBC) are taken into account.

$$I_i^k = I_i^r(V_i^k) + jI_i^i(V_i^k) = \left(\frac{P_i + jQ_i}{V_i^k} \right) \quad (8)$$

Where V_i^k and I_i^r are respectively the bus voltage and the equivalent i^{th} bus current injection at k^{th} the iteration. I_i^r And I_i^i are respectively the real and imaginary parts of the equivalent current injection of bus i at iteration k^{th} . Figure 1 below is an example of radial distribution system.

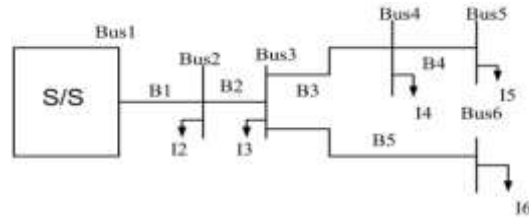


Fig. 1: Example of radial distribution system

From equation 2, the injected currents are obtained. By applying Kirchhoff's current law (KCL) to the distribution network, the current branches are calculated. A simple distribution system, shown in Figure 1, is used as an example test system. Bypass currents can be formulated based on equivalent current injections. The bypass currents B_1, B_2, B_3, B_4 and B_5 can be expressed as follows:

$$B_1 = I_2 + I_3 + I_4 + I_5 + I_6$$

$$B_2 = I_3 + I_4 + I_5 + I_6$$

$$B_3 = I_4 + I_5$$

$$B_4 = I_5$$

$$B_5 = I_6$$

$$[BCBV] = \begin{bmatrix} Z_{12} & 0 & 0 & 0 & 0 \\ Z_{12} & Z_{23} & 0 & 0 & 0 \\ Z_{12} & Z_{23} & Z_{34} & 0 & 0 \\ Z_{12} & Z_{23} & Z_{34} & Z_{45} & 0 \\ Z_{12} & Z_{23} & Z_{34} & Z_{45} & Z_{56} \end{bmatrix}$$

The general form of the bus voltage at $(k+1)$ th iteration can be expressed as

$$V^{k+1} = [V_1] - [BCBV][B] \quad (9)$$

In general form, with i and k denoting the node and iteration number respectively

$$I_{i-1,i}^k = I_i^k + I_{i,i+1}^k \quad (10)$$

$$V_i^k = V_{i-1}^k - Z_{i-1,i} * I_{I-1',I}^{k-1} \quad (11)$$

$$\Delta V = \sqrt{3} \sum_{i=1}^n I_i (R_i \cos \theta + X_i \sin \theta) L_i \quad (15)$$

4.2 Procedure to form the BIBC and BCBV matrix

As seen above, the BIBC and BCBV matrices are developed based on the topological structure of the distribution systems. The BIBC matrix represents the relationship between bus current injections and bypass currents. The corresponding variations in branch currents, generated by variations in bus current injections, can be calculated directly by the BIBC matrix. The BCBV matrix represents the relationship between shunt currents and bus voltages. The corresponding variations in bus voltages, generated by variations in branch currents, can be calculated directly by the BCBV matrix. Thus, the BIBC and BCBV training procedures are presented below[18].

Step 1: For a distribution system with a branch section m and a bus n, the dimension of the BIBC matrix is mx (n-1).

Step 2: If a line section (B k) is located between bus i and bus j, copy the column of the i th bus from the BIBC matrix into the column of the j th bus and fill in a 1 at the position of k th line and the jth bus column.

Step 3: Repeat step (2) until all row sections are included in the BIBC matrix.

4.3 Power loss calculation

Line losses can be calculated in the distribution system in primary and secondary feeders. The active and reactive power loss in the distribution system per phase can be calculated as follows:

$$P_{loss} = \sum_{i=1}^{nb} |I(i)|^2 * R(i) \quad (12)$$

$$Q_{loss} = \sum_{i=1}^{nb} |I(i)|^2 * X(i) \quad (13)$$

The total active and reactive power loss of the distribution systems is obtained by adding the losses of each branch current line:

$$P_{TLoss} = \sum_{t=1}^{nb} P_{Loss}(t, t+1) \quad (14)$$

4.4 Voltage drop calculation

All equipment connected to the electrical network is designed to be used under a certain defined voltage. It is not practical to serve every customer on an electrical distribution at the same voltage exactly matching the nameplate voltage, because voltage drops exist in every part of the electrical system, from generation to the customer's meter. The voltage drop in the distribution system can be calculated as follows [19].

4.5 Load flow with D- STATCOM

D-STATCOM is a shunt device that uses force-switched power electronics to control power flow and improve transient stability on power networks. It is also part of the so-called flexible AC transmission system devices. The D-STATCOM is a three-phase shunt-connected Voltage Source Converter (VSC), designed for use in the distribution network to compensate for bus voltage to provide better power factor and reactive power. The device is capable of injecting or absorbing active and reactive current at the point of common coupling (PCC). The limiting constraint linked to energy storage makes it practically impossible for D-STATCOM to inject active power over a long period. Thus, operation is primarily steady state, with reactive power being the power exchange between D-STATCOM and the system. Figure 2 shows a schematic diagram of D-STATCOM incorporated into a k bus [20].

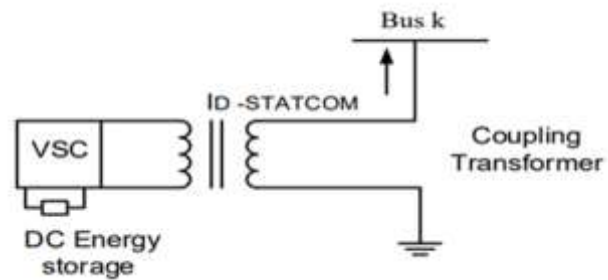


Fig. 2: D-STATCOM connected to a certain bus k [20]

4.6 Components of D-STATCOM

D-STATCOM consists of a three-phase inverter (usually a PWM inverter) using SCRs, MOSFETs or IGBTs, a DC capacitor which supplies the DC voltage to the inverter, a link choke which connects the output of the inverter to the AC power side, a filter Components to filter high frequency components due to the PWM inverter. From the DC side capacitor, a three-phase voltage is generated by the inverter. This is synchronized with AC power. The link inductor connects the system voltage to the AC power side [21].

4.7 Basic working principle of D-STATCOM

The voltage of the D-STATCOM is injected in phase with the mains voltage and in this case, there is no energy exchange with the network, but only the reactive power is to be injected (or absorbed) by the D-STATCOM. The reactive power exchange with the network is achieved by varying the amplitude of the output voltages. The output voltage of Vd is controlled in phase with the system

voltage V_s . If V_d is greater than V_s then the D-STATCOM will act as a capacitor and generate reactive power (capacitive mode). On the other hand, if V_s is greater than V_d then the D-STATCOM will act as an inductor and consume reactive power (inductive mode). If V_d is equal to V_s then D-STATCOM neither generates nor absorbs reactive power and the reactive power is zero (no-load mode)[22].

4.8 Applications of D-STATCOM

D-STATCOMs are typically used in long distance transmission systems, electrical substations and heavy industries where voltage stability is the primary concern. Furthermore; Synchronous static compensators are installed at selected points in the electrical system to perform the following basic functions. The basic functions of D-STATCOM include: Voltage regulation and reactive power compensation of harmonic currents. Power factor correction, Voltage flicker mitigation and uninterrupted power supply when used as an energy storage device[14].

4.9 Reasons to choose D-STATCOM

There are two main conventional ways of controlling voltage on distribution systems: Series voltage regulator and shunt capacitors are the two conventional ways of keeping distribution system voltages within an acceptable range, but these devices have some disadvantages that conventional series voltage regulators cannot generate reactive power and have quite slow response due to their step-by-step operations. The reason why D-STATCOM was chosen as a compensation device over other FACTS shunt equipment is: to autonomously control the voltage, resulting in much faster power factor correction. continuously variable output without steps, without harmonics, without transients, it can generate and absorb reactive power and reacts practically instantly [23].

4.10 D-STATCOM modeling

The steady-state mathematical modeling of D-STATCOM is explained as follows. A simple two-bus radial distribution system is shown in Figure 3.

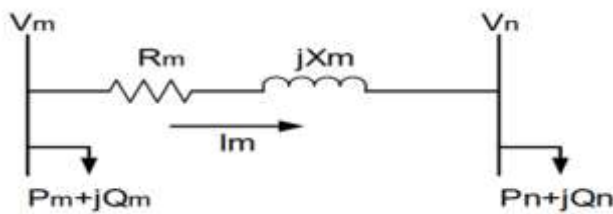


Fig. 3: Two-bus radial distribution system
The voltage equation for the two-bus system is given as follows

$$V_n = V_m \angle \theta_m - (R_m + jX_m) I_m \angle \delta \quad (16)$$

The schematic of two-bus radial distribution system with D-STATCOM is shown in Figure 4.

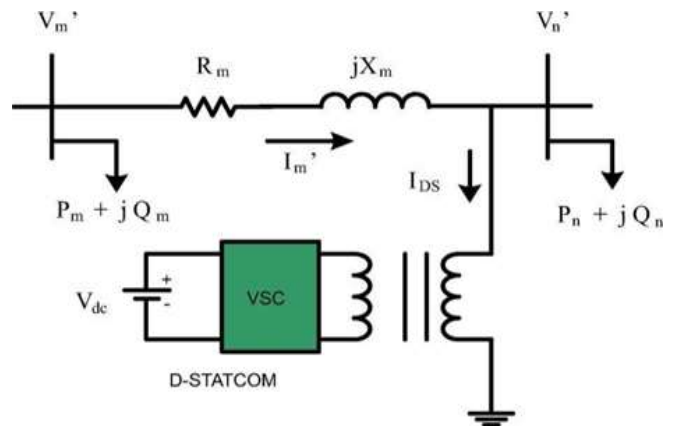


Fig. 4: Two-bus radial distribution System with D-STATCOM

By installing D-STATCOM, the voltage values on the bus where it is installed and on the neighboring bus change.

The new tensions are V'_n on the candidate bus and V'_m on the previous neighboring buses. The current changes and I'_m corresponds to the sum of I_m and I_{DS} . Here, I_{DS} is the current injected by D-STATCOM and is in quadrature with the voltage. Therefore, the expression of the new voltage after installing D-STATCOM is given as follows:

$$V'_n \angle \theta'_n = V'_m \angle \theta'_m - (R_m + jX_m) \left(I_m \angle \delta + I_{DS} \angle \left(\frac{\pi}{2} + \theta'_n \right) \right) \quad (17)$$

Here θ'_n , θ'_m and δ are the phase angles of V_n , V'_m and I_m respectively. Separating the real and imaginary parts of the above equations, we obtain

$$V'_n \cos \theta'_n = \text{Real}(V'_m \angle \theta'_m) - \text{Real}(Z_m I_m \angle \delta) - R_m I_{DS} \cos \left(\frac{\pi}{2} + \theta'_n \right) + X_m I_{DS} \sin \left(\frac{\pi}{2} + \theta'_n \right) \quad (18)$$

$$V'_n \sin \theta'_n = \text{Imag}(V'_m \angle \theta'_m) - \text{Imag}(Z_m I_m \angle \delta) - R_m I_{DS} \sin \left(\frac{\pi}{2} + \theta'_n \right) + X_m I_{DS} \cos \left(\frac{\pi}{2} + \theta'_n \right) \quad (19)$$

So the bus voltage angle is

The current angle and amplitude of the D-STATCOM are

$$\angle I_{DS} = \frac{\pi}{2} + x_2 = \frac{\pi}{2} + \sin^{-1} t \quad (20)$$

$$|I_{DS}| = x_1 = \frac{V_n \cos \theta_n - h_1}{-h_4 \sin \theta'_n - h_3 \cos \theta'_n} \quad (21)$$

Finally, the reactive power injected is:

$$jQ_{DS} = (V'_n \angle \theta'_n) \cdot \left(I_{DS} \angle \left(\frac{\pi}{2} + \theta'_n \right) \right) \quad (22)$$

Where * denotes the conjugated complex.

5 Optimization technique used to solve power loss and voltage drop

Optimization consists of finding the best solution to a problem under predefined constraints. Intelligent techniques such as bee colony, particle swarm, firefly, cuckoo search, ant lion, genetic algorithm, whale optimization, simulated annealing and harmony search have been applied to incorporate shunt compensation devices into electrical distribution systems. Recent efforts have focused on solving the problem of optimal placement of fact devices.

5.1 Analytical methods

Although analytical methods suffer from many drawbacks, they are still used to optimize the location and size of FACTS in distribution systems. Indeed, they are easy to use and their logical analysis can be easily followed[24] .

5.2 Computational methods

Although these methods are fast compared to other classes of techniques, their disadvantage is that they are complex and reproducing their results can be difficult, or sometimes impossible[25] .

5.3 Artificial intelligence methods

Artificial intelligence (AI) is increasingly being used to solve optimization problems, with techniques such as particle swarm optimization (PSO) and genetic algorithms (GA) under development. These methods aim to obtain more precision in the optimization process. PSO is chosen as the most effective technique to optimize the location and size of FACTS in power distribution systems, ensuring reduced power losses and improved voltage profiles [25] . Researchers used PSO as an optimization technique for exploration, followed by an improved version incorporating crossover and mutation parameters for exploitation. They compared GA and PSO to resolve distribution losses and distribution line voltage deviations. The theoretical background of the most used optimization algorithms is discussed below [25] .

5.3.1 Particle Swarm Optimization

Particle swarm optimization is a population-based meta-heuristic optimization approach, created in 1995 by James Kennedy and Russell Eberhart and motivated by flocks of birds or schools of fish[26] . PSO is initialized with a random number of solutions called particles which are left free on a “search space”. Each particle is a possible solution to the problem and has a fitness value. Physical condition is assessed and must be optimized. A velocity is defined that directs the position of each particle and is updated with each iteration. The particles end up moving towards the optimum due to their best location and the best solution this group has ever encountered. A particle's velocity is updated based on three factors: the particle's

previous velocity, the best position the particle has ever been in, and the best position the entire swarm has ever been in[27] . Particles track their coordinates in the search space, linked to their best solution (fitness) so far. Personal best (Pbest) and Gbest (best value) are tracked by the Particle Tracking System (PSO). PSO uses random weighted acceleration to accelerate particles toward their Pbest and Gbest positions at each time step. The dominant speed is calculated using the previous speed and distance between Pbest and Gbest [27] .

$$V_{id}^{k+1} = wV_{id}^k + c_1r(P_{bestid} - S_{id}^k) + c_2r(G_{bestid} - S_{id}^k) \quad (23)$$

$$S_{id}^{k+1} = S_{id}^k + V_{id}^{k+1} \quad (24)$$

Where $i=1, 2, \dots, n$ & $d=1, 2, \dots, m$
The following weight function is used

$$W_k = W_{max} - \left(\frac{W_{max} - W_{min}}{K_{max}} \right) \cdot k \quad (25)$$

Where W_{min} , and W_{max} are the minimum and maximum weights respectively. K and K_{max} are the current and maximum iteration.

How particles update their speed in a PSO is indicated in Figure 5.

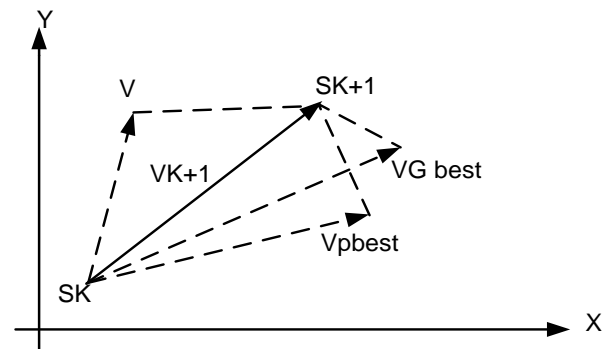


Fig. 5: Updating Speed in PSO

5.3.1.1 PSO parameter selection and optimization process

For any given optimization problem, certain parameters of the PSO algorithm can affect its effectiveness. Certain values and choices of these parameters have a significant impact on the performance of PSO techniques, while others have little or no impact. The basic parameters of PSO are [27] :

Swarm size refers to the number of agents in a swarm, with larger swarms generating more particles and covering more search space per iteration. Reducing the number of iterations can increase the computational complexity and time consumption. The particle velocity is constrained by the parameters, which determine the resolution or adequacy of the regions between the current and target positions. High V_{idmax} can cause particles to overtake good solutions, while low V_{max} can cause particles to take longer to reach the desired solutions.

Speed components play a crucial role in updating an agent's speed, with three terms: inertia, cognitive, and social. Inertia provides information about the agent's recent history, while cognitive measures performance based on past performance. Social measures performance based on a group of agents, guiding each agent to the best position found by their neighborhood.

The accelerating coefficients C1 and C2 play a crucial role in determining the optimal values for the PSO. Initialization of C1 and C2 is crucial to obtain the optimal values, and incorrect assumptions can result in cyclical behavior. It is recommended to use C1 and C2 = 2 for optimal results[27].

Inertia Weight: The inertia weight determines how much of the previous time step's velocity should be retained. However, the best results were obtained by adopting an inertia mass that increases from 0.9 to 0.4 throughout the first simulation course. This setting allows the PSO to search a large region at the beginning of the simulation when the inertia weight is high, and then refine the search later when the inertia weight is lower. Another advantage of adopting a decreasing inertia mass is that it damps the oscillations of particles close to gbest. Additionally, damping particle oscillations around gbest is another advantage obtained by using decreasing inertia mass. These oscillations are recorded when a large constant inertial mass is used. As a result, removing these oscillations helps the particles in the swarm converge toward the best overall solution. According to, the value of inertia weight (w) should drop linearly from 0.9 to 0.4 during the experiment [27].

In general, the inertia weight (w) is adjusted according to equation (2.3) above. The appropriate values for w_{min} and w_{max} are 0.4 and 0.9, respectively. **Termination Criterion:** After the initial phase, several iterations of update and evaluation steps are performed until a termination condition is met. Generally, the stopping condition is the achievement of a predefined maximum number of iterations or the achievement of a certain precision in the solution. PSO has the following advantages including [27].

1. PSO is based on swarm intelligence. It can be applied to both scientific research and engineering.
2. PSO has the advantage of fast convergence rate compared to most optimization techniques, including genetic algorithm.
3. PSO has no overlap or mutation calculation. The velocity of the particle can be used to perform the search, for example relative to GA.
4. PSO has a stronger memory capacity than GA since each particle remembers its own previous best value as well as the neighboring best value.
5. PSO is more effective at maintaining swarm diversity than GA because bad solutions are discarded and only good ones are kept, resulting in a population that revolves around a subset of the best individuals because all particles use the information from the most successful particle to improve. The main disadvantages of PSO are:

1. The approach is prone to partial optimism, which causes it to be less precise in regulating its speed and direction.

2. The method may not properly solve the problems of the uncoordinated system, such as the solution to the energy field and the Variable rules of particles in the energy field. In the PSO algorithm, the population has n particles which represent candidate solutions. Each particle is a real-valued vector of m dimensions where m is the number of optimized parameters. Therefore, each optimized parameter represents one dimension of the problem space [27]. The proposed PSO technique for the optimization algorithm is described using the following steps and shown in Figure 6.

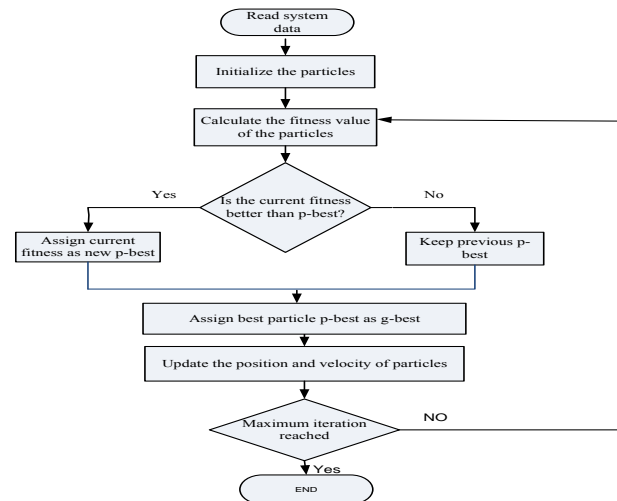


Fig.6: PSO optimization flow chart

Step 1: Initialization: Set all parameters and generate n random particles, each particle in the initial population is evaluated using the objective function f . Set iteration counter $k = 1$. Randomly generate an initial population (array) of n particles. The initial velocity of each particle is randomly generated for the evaluation of the objective function. K_{max} , W_{in} , W_{max} , C_1 and C_2 are assigned. In this step, the lower and upper bounds of the regional constraints are also specified.

Step 2: Calculate the objective function: Calculate the objective function and find the fitness value of each particle.

Step 3: Comparison of fitness values: The fitness value of each particle in the first iteration becomes its best p . In the previous iteration, if the new value of p best is obtained as well as the previous one, it is modified otherwise it remains the same.

Step 4: Assign the best personal value as the best overall value: The best fitness value among all P bests is denoted by G best.

Step 5: Changing the Speed: Change the speed of each particle using the following equation:

Then generate the new particles based on the following equation:

$$S_{id}^{k+1} = S_{id}^k + V_{id}^{k+1} \quad (26)$$

$i=1, 2, \dots, n$ and $d=1, 2, \dots, m$

Step 6: Update Iterations: Update the iteration counter, $k = k+1$.

Step 7: If the stopping criteria are met, go to step 8, otherwise go to step 2.

Step 8: Stop. The particle that generates the last iteration is the optimal PSO solution

5.3.1.2 Benefits of PSO

1. Based on swarm intelligence. It can be applied to both scientific research and engineering.
2. PSO has the advantage of fast convergence rate compared to most optimization techniques, including genetic algorithm.
3. PSO has no overlap or mutation calculation. The search can be done by the velocity of the particle, for example in comparison with GA.
4. During the development of several generations, only the most optimistic particle can transmit information to other particles, and the search speed is very fast.
5. The calculation in PSO is very simple. Compared to other calculations in development, it occupies a larger optimization capacity.
6. PSO adopts the actual digital code, and it is decided directly by the solution. The dimension number is equal to the solution constant. The main disadvantages of PSO are:
 1. The method easily suffers from partial optimism, which makes the regulation of its speed and direction less precise.
 2. The method may not properly solve problems of uncoordinated systems, such as the solution of the energy field and the rules for moving particles in the energy field.

6 Case study

Woldya, located in the northern part of Ethiopia, is one of the oldest cities in the country. The city has many shopping centers, small industries and densely populated residents. The old and mobile substations of Woldya are structured to supply the city. An incoming 230KV line from the Dorogbir mobile substation and an incoming 66KV line are fed from the Dessie substation. These two substations have a total of thirteen feeders, seven of which are 15KV feeders and the rest are 33KV feeders.

The data required for this thesis work was collected from Woldya distribution substation, Ethiopian Electric Utility (EEU) engineering office and Ethiopian Electric Power (EEP). The data was collected from the recorded feeder loading data (peak load) of the substation and the conductor impedance and other important data are collected.

1. Old Woldya substation: This substation is located at kebele-03, near Woldya bus station. It has a dual bus bar system comprising a single transformer with 6.3/8.4 MVA, 66/15 KV and 8.4 MVA, 66/33/15 KV three-phase transformers. There are three 15KV feeders and three 33KV feeders in this substation.
2. New Woldya substation: it has two 230/33/15KV power transformers with a nominal power of 50MVA each and supplies four 15KV feeders and three 33KV feeders. The substations can be modeled using Microsoft Office Visio

software and the single line diagram is shown in Figure 7 below combining the two substations.

6.1 Analysis of the loading capacity of existing Woldya 15 and 33KV power lines

All existing feeder lines in the city are used to distribute medium voltage level of 15 and 33 KV from substations to distribution centers over long distance coverage. According to substation data, both substations operate with a power factor of 0.8. Peak load power (MW) and peak load current (A) data are available and the maximum reactive power load can be calculated using the following equations.

$$S = \sqrt{P^2 + Q^2} \quad (27)$$

$$P = \sqrt{3}VI \cos \theta \quad (28)$$

$$Q = \sqrt{3}VI \sin \theta \quad (29)$$

Where: P, Q and S are respectively the active, reactive and apparent powers, V is the starting voltage 15KV; I is the current reading and $\cos \theta$ power factor of the substation. Among the thirteen 15 and 33 KV feeders of the Woldya Distribution substation, the Gonder ber feeder (F 7) is selected for this case study for the following reasons: high energy demand, high peak load current, long distance covered and departure Gonder ber has 69 knots, and a total capacity of 7.2 MW.

6.2 Gonder ber Distributor Analysis

Gonder ber feed emanates from Dorogbir mobile substation and this feed is one of the heavily loaded feeds of Woldya town covering large areas from Dorogbir to Gonder ber up to Tikur Wuha River. In this area there are some load centers which require very reliable energy like health station, oil factory, Yeju mars Process, Poly technic collage, Teacher College, milk processes, Mifa powder factory, Yeju powder factory, Yegna plastic factory and small industry etc.

6.3 Bus and branch numbering system

The bus and branch numbering system is very important for the study of a given electrical system. Even though the numbering scheme has no effect on the calculation efficiency of departures, it must be assigned schematically, including the laterals. It starts from the substation by assigning it the bus number 1. The departures starting from the substation and going to the ends are main departures while the branches emanating from the main departure and not from the substation are called lateral. For example, in Figure 7, is the single-line schematic representation of the Gonder ber charger drawn using Microsoft Office Visio.

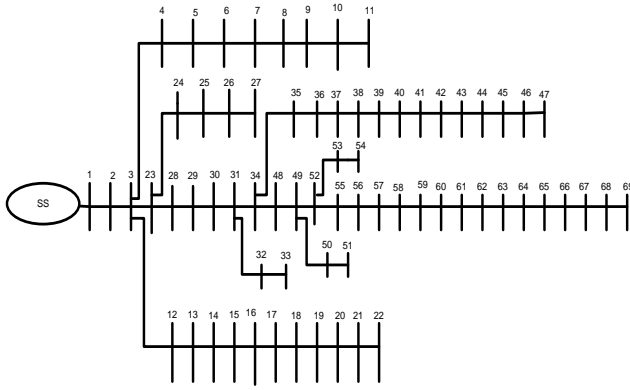


Fig. 7: Single-line diagram of the Gonder ber distributor

6.4 per-Unit value (p.u)

It is a dimensionless value of any quantity obtained by dividing the actual value by the base value in the same unit. This makes the calculation easier since all values are taken in the same unit (p.u).

$$\text{Unit value} = \text{Actual val.} / \text{Base val.} \quad (30)$$

Based on the basic base values (S base, and V base), the derived base values can be

$$I_{base} = \frac{S_{base}}{V_{base}} \quad (31)$$

$$Z_{base} = \frac{V_{base}^2}{S_{base}} \quad (32)$$

Now taking the common base power (100 MVA) and system voltage (15 KV) as base values

$$I_{base} = \frac{S_{base}}{V_{base}} = \frac{100MVA}{15KV} = 6.6667KA \quad (33)$$

$$Z_{base} = \frac{V_{base}^2}{S_{base}} = \frac{(15KV)^2}{100MVA} = 2.25\Omega \quad (34)$$

The ratio of active power to base power and reactive power to base power gives the unit values of active and reactive power respectively.

6.5 Overhead line impedance calculation

The inductance of a transmission line depends on the material, dimensions and configuration of the wires and the length and spacing between them. A conductor's AC resistance is always greater than its DC resistance due to the skin effect forcing more current near the exterior. Conductor surface. The higher the frequency of the current, the more noticeable the skin effect will be. Wire manufacturers usually provide tables of resistance per unit length at common frequencies (50 or 60 Hz). The conductors used in distribution feeders are stranded

conductors. The inductive reactance is calculated at a frequency of 50 Hz and over a length of one kilometer. . Thus, the impedances are given by [28] .

$$Z_a = R_a + j0.06283 \ln \frac{D}{GMR} \Omega / km \quad (35)$$

$$GMR = k.r \quad (36)$$

$$D = \sqrt[3]{D_{ab}D_{bc}D_{ac}} \quad (37)$$

6.6 Sixty Nine Bus Gonder ber Radial Distribution Distributor

It consists of a total number of sixty -nine power buses of which bus-1 is taken as the reference node or slack bus, 11 nodes are common coupling nodes and 57 nodes are connected to the loads through a transformer of step-down distribution. The single line diagram of the Gonder feeder is shown in Figure 3.2. The power line is a stranded conductor of type AAC-50 and AAC-95 with a total length of 31.2 km. These overhead lines are used to distribute medium voltage power (15 kV) from Woldya Mobile Substation to distribution transformers.

7 Result and Discussion

In this section, the results obtained using the load flow, PSO and VSI methods were presented. The algorithm described in the previous section is applied and programmed in Mat lab 2019a. The implementation parameters of the PSO algorithm are shown below in the Table 1:

Table 1. Parameter value for PSO simulation

Population Size	Number of iterations	W _{min.}	W _{max.}	C1	C2
40	20	0.4	0.9	2	2

Based on the collected data, a backward sweeping load flow algorithm was performed, and from there, the preliminary power loss, bus voltage and voltage stability index of the feeder had been obtained. To obtain the best location and size of D-STATCOM, a bus-based voltage stability index analysis guided by the PSO algorithm was simulated. The simulation results for the suggested system are tested in four cases: Case 1: system without D-STATCOM, Case 2: system with only one D-STATCOM

7.1 Case 1: System without D-STATCOM

The base case real and reactive power losses, voltage profile and voltage stability index of the Gonder ber feeder were simulated via Mat lab Software. The actual power loss, reactive power loss, minimum voltage amplitude,

minimum voltage stability index amplitude of the charger are 172.8202 kW, 42.4213 KVAR, 0.9453pu and 0.7985 P.u without installing D-STATCOM. The base case voltage profile and stability index are shown in Figures 8 and 9, respectively.

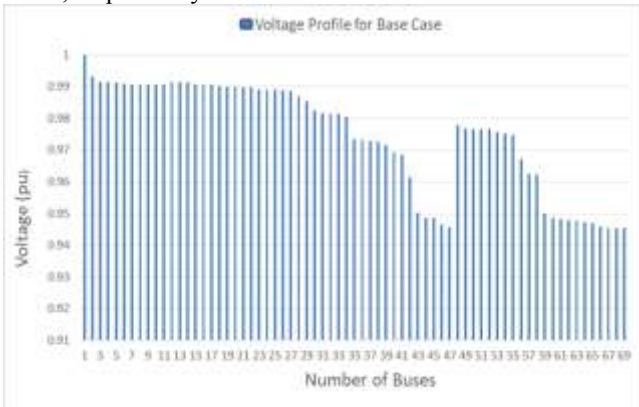


Fig. 8: Voltage profile for the base case scenario

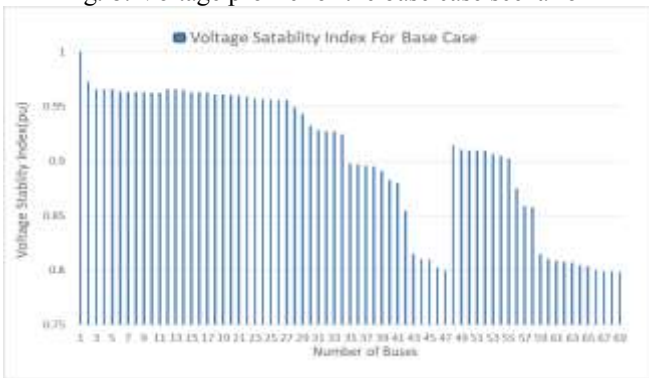


Fig. 9: Voltage stability index for the base scenario

7.2 Case 2: System with a single D-STATCOM

In case 2, the real and reactive power losses, voltage profile and voltage stability index of the Gonder ber feeder were simulated. The actual power loss, reactive power loss, minimum voltage amplitude and minimum voltage stability index amplitude of Gonder ber charger are 35.8184 kW, 29.4665 KVAR, 0.9802pu respectively and 0.9230 P.u with single installation of D-STATCOM. The voltage profile of Case 2, stability index, active power loss and reactive power loss are shown in Figures 10, 11, 12 and 13, respectively.

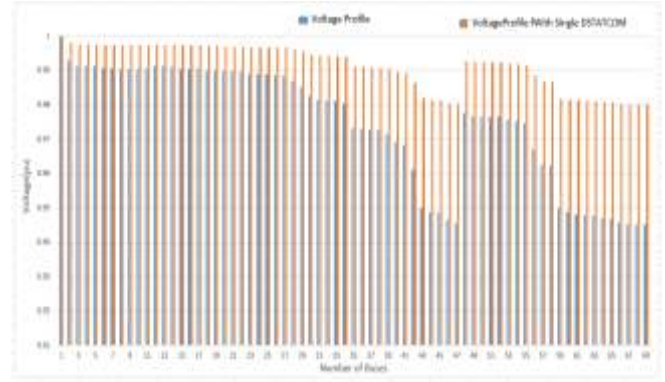


Fig. 10(a): Voltage profile without and with D-STATCOM

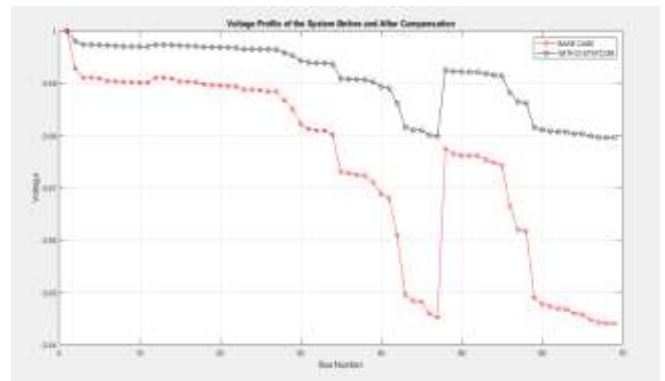


Fig. 10(b): Voltage profile without and with D-STATCOM

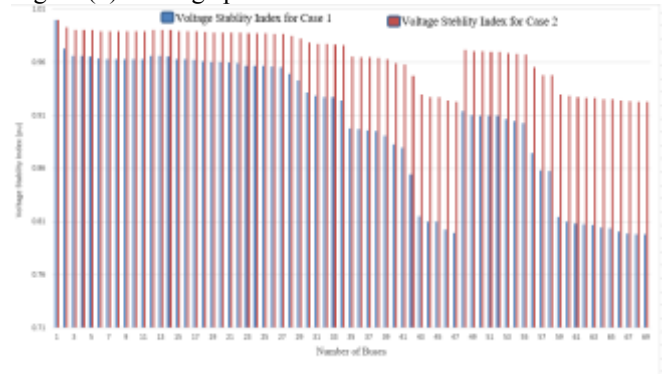


Fig. 11(a): Voltage stability index without and with D-STATCOM

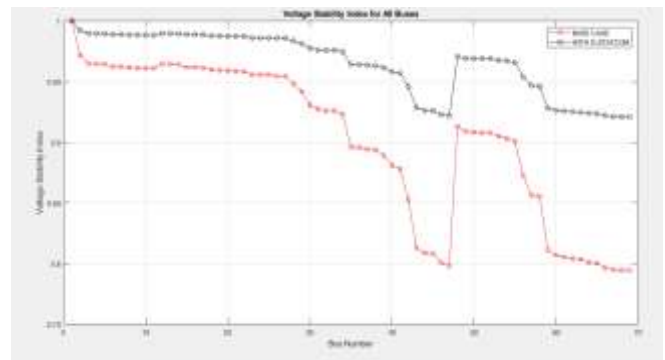


Fig. 11(b): Voltage stability index without and with D-STATCOM

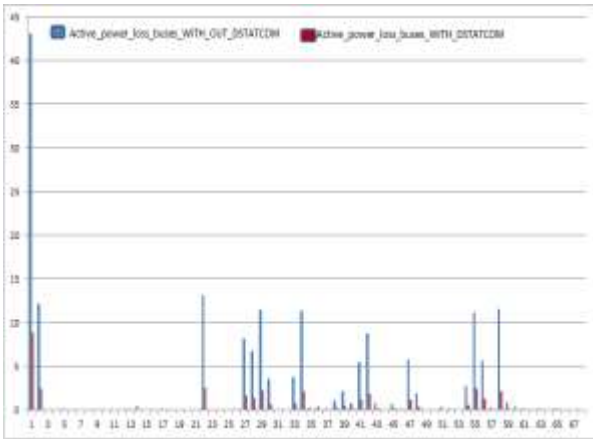


Fig. 12(a): Active power loss of all buses for case 2

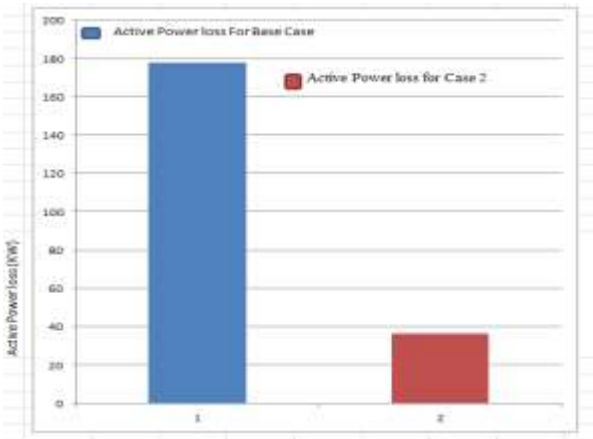


Fig. 12(b): Active power loss before and after compensation for case 2

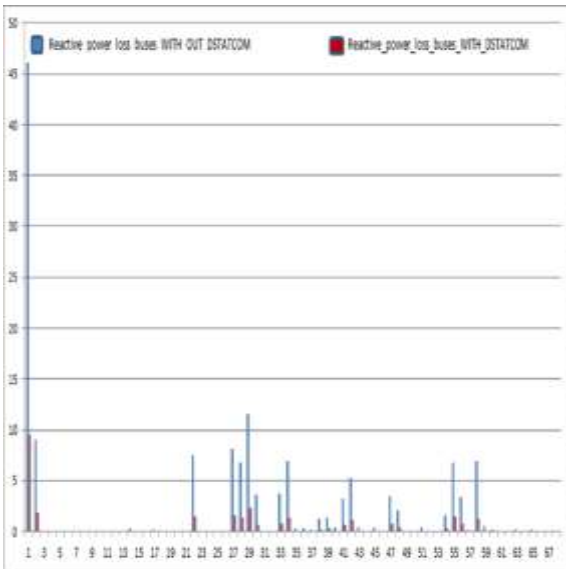


Fig. 13(a): Reactive power loss of all buses for case 2

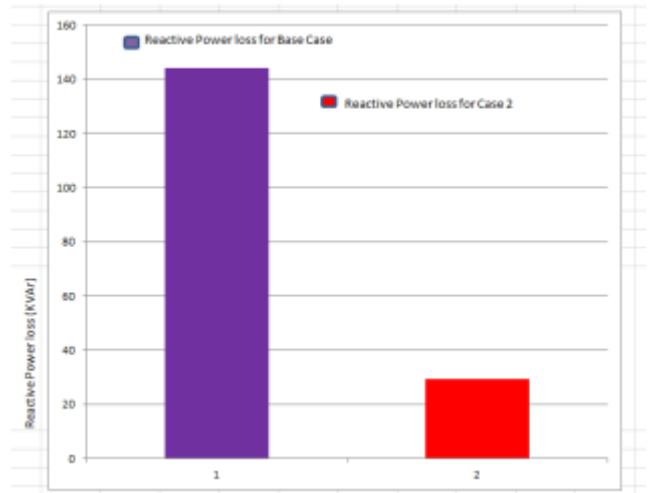


Fig. 13(b): Reactive power loss before and after compensation for case 2

Table 2, shows that the comparison of real power loss, reactive power loss, voltage profile, voltage stability index, location, optimal size of the D -STATCOM, of the percentage reduction in active and reactive power losses for case 2.

Table 2. Performance evaluation for Case 2

No	Parameters	Base case	PSO (Case 2)
1	Loss of active power	177.9424KW	36.4801KW
2	Loss of reactive power	144.2124 KVA	29.5017 KVA
3	Minimum VSI	0.7942pu	0.9193pu
4	Minimum voltage	0.9440pu	0.9792pu
5	Location of D-STATC	@ Bus number 1
6	Size D-STATCM	1250KVA
7	% active power loss	79.498900
8	% reactive power loss	79.542900

8. Conclusion

This paper demonstrates the effectiveness of a PSO optimization technique to reduce system power loss, improve voltage profile, and increase voltage stability index by optimizing the location and size of D-STATCOM. The bus-based voltage stability index was used to reduce the search space of the algorithm. A direct load flow analysis method was applied to determine system voltage and active and reactive power losses. A multi objective function was formulated for the optimization algorithm, which was tested on the Woldya Gonder ber Feeder (F7). The simulation results showed a significant reduction in real power losses and reactive power losses, resulting in a total annual cost reduction of 1,478,771.22 Birr and a payback period of 1.8 years. A

Sino pack company offered a better price for a D-STATCOM supplier of size 1250KVAR, which resulted in a total installation and the price of D -STATCOM is 2,652,242.857 Birr.

References

- [1] HM Daealhaq, YF kfajey and AS Tukkee, "Reducing power losses and improving voltage profile using an optimal ater. Sci. Eng., flight. 1067, no. 1, p. 012128, 2021, doi: 10.1088/1757-899.
- [2] H. Singh and S. Garg, "Improving voltage profile and reducing line losses using DG using GSA and PSO optimization techniques," J.Res., vol.03, no.01, pp.6670, 2017, [Online]. Available :www.journal4research
- [3] T. Hambissa, "Addis Ababa Institute of Technology, School of Electrical and Computer Engineering, Addis Ababa Institute of Technology, School of Electrical and Computer Engineering," no. March, pp. 1-32, 2017.
- [4] IV Tuzikova and Prague, "The use of evidence-based technologies to minimize power losses and improve energy stability in power grids", Doctoral thesis Dep. Electr. Power engineering. Czech technology. Univ. Prague Fac., No. August, p.
- [5] R. S. Wibowo, S. Member, N. Yorino, and M. Eghbal, "Allocation of FACTS devices with control coordination considering congestion relief and voltage stability," vol. 26, no. 4, pages 2302 to 2310, 2011.
- [6] PS Engineering, "Study and Improvement of Power Distribution System Performance Using D-STATCOM (Case Study: Gondar City Distribution Network)", 2022.
- [7] Nebiyu, "Loss Reduction and Voltage Stability Improvement of Distribution Network through Optimal Allocation of Distribution Statcom Case Study (Bahir Dar Distribution Network)", 2020.
- [8] J. Romero Aguero, "Improving the efficiency of energy distribution systems through the reduction of technical and non-technical losses," Proc. IEEE power engineering. Soc. Transm. Distribute. Conf., pp. 1-8, 2012, doi: 10.1109/TDC.2012.6281652.
- [9] Wondwossen A. H., Chandrasekar Perumal. "Design and performance analysis of hybrid micro-grid power supply system using Homer software for rural village in Adama area, Ethiopia". International Journal of Scientific & Technology Research, Vol.8 No.6, P. 267-275, 2019.
- [10] RK Bindal, "A Review of the Benefits of FACTS Devices in Power System," Ijeat, vol. 3, no. 4, p. 105-108, 2014.
- [11] B. Adebajji, W. Akinyele, J. Femi-Jemilohun, C. Okafor and I. Ismail, "Reduction of power losses and improvement of voltage profile in electric power distribution networks using of static var compensators", Int. J. Adv. Sci. Eng. Inf. Technology.
- [12] B. Adebajji, W. Akinyele, J. Femi-Jemilohun, C. Okafor and I. Ismail, "Reduction of power losses and improvement of voltage profile in electric power distribution networks using of static var compensators", Int. J. Adv. Sci. Eng. Inf. Technology. , flight. 11, no. 5, pp. 1763-1771, 2021, doi: 10.18517/ijaseit.11.5.11830.
- [13] S. Gade, R. Agrawal, and R. Munje, "Recent trends in power quality improvement: review of the unified power quality conditioner," ECTI Trans. Electr. Eng. Electron. Common., flight. 19, no. 3, pp. 268-288, 2021, doi: 10.37936/ecti-eec.2021193.244936.
- [14] Mokhtari, FZ Gherbi, C. Mokhtar and DE Kamel, "Study, analysis and simulation of a static compensator D-STATCOM for electrical power distribution systems", Leonardo J. Sci., No. 25, p. 117-130, 2014.
- [15] Masashi Asakura, "No subjective feeling of health among elderly people living at home. Analysis of the covariance structure for health-related indicators Title", Carbohydr. Polym. , flight. 6, no. 1, pp. 5-10, 2019.
- [16] PALDG Gowtham, "Power loss reduction and voltage profile improvement by DSTATCOM using PSO," Int. J. Eng. Res. Technol., flight. 4, no. 2, pp. 553-557, 2015, [Online]. Available: www.ijert.org
- [17] A, de Almeida, L. Moreira and J. Delgado, "Power quality problems and new solutions," Renew. Energy Power Qual. J., vol. 1, no. 1, pp. 25-33, 2003, doi: 10.24084/repqj01.004.
- [18] G. Peddanna and C. Rajesh, "Power Loss Reduction Index for Radial," pp. 7559-7564, 2016, doi: 10.15662/IJAREEIE.2016.0509060.
- [19] N. Al Masood, A. Jawad, K. T. Ahmed, S. R. Islam, and M. A. Islam, "Optimal placement of capacitors in northern region of Bangladesh transmission network for improvement of voltage profile," Energy Reports, vol.. 9, pp. 1896-1909, 2023, doi: 10.1016/j.egy.2023.01.020.
- [20] S. Do Nascimento and MM Gouvêa, "Improving voltage stability in power systems with automatic allocation of fact devices," Energy Procedia, vol. 107, no. September 2016, pp. 60-67, 2017, doi: 10.1016/j.egypro.2016.12.129.
- [21] SA Basha and YB Raju, "Transient Stability Performance Analysis of Multi-Machine Power System Using Facts Device," Int. J. Electr. Electron. Eng., flight. 5, no. 7, pp. 9-15, 2018, doi:10.14445/23488379/ijeee-v5i7p103.

- [22] K. Mehra and R. Kaur, "D-STATCOM for Power Quality Improvement in Power Distribution Systems Using MATLAB Simulink," *Int. Res. J.Eng. Technology*, 2020, [Online]. Available: www.irjet.net
- [23] R. Dhakar, "Brief summary document on DSTATCOM for improving power quality", vol. 6, no. 3, p. 171-178, 2021.
- [24] HR Kolatel, HH Kolate and PP Khampariya, "A review paper on power quality improvement and case study on mitigation using power flow controller distributed", vol. 4, no. 4, p. 606-610, 2016.
- [25] Ismail, NI Abdul Wahab, ML Othman, MAM Radzi, K. Naidu Vijyakumar and MN Mat Naain, "A comprehensive review on optimal location and sizing of reactive power compensation using Hybrid Approaches for Power Loss Reduction, Voltage Stability Enhancement, Voltage Profile Enhancement, and Load Capacity Enhancement," *IEEE Access*, vol. 8, pp. 222733-222765, 2020, doi: 10.1109/ACCESS.2020.3043297.
- [26] H. Amulya, T.M. Kumar and K. Mohan, "Application of PSO and GA in Optimal Placement of FACTS Devices in Transmission Line," *Int. J. Curr. Eng. Technology.*, flight. 4, no. 3, pages 1977-1981, 2014.
- [27] YT GEBREYES, "Studies on voltage control of distribution substations using static var compensators", n° 26. January, p. 1 to 88, 2019.
- [28] SM Vera, I. Nuez and M. Hernández-Tejera, "A FACTS device allocation procedure for load sharing," *Energies*, vol. 13, no. 8, pp. 1-16, 2020, doi: 10.3390/en13081976.

Contribution of individual authors to the creation of scientific article

The authors equally contributed to the present research, at all stages from the formulation of the problem to the final findings and solution.

Sources of funding for research presented in a scientific article or scientific article itself

No funding was received for conducting this study

Conflict of interest

The authors have no conflicts of interest to declare that are relevant to the content of this article.

Creative commons attribution licence 4.0 (attribution 4.0 international, CC BY 4.0)

This article is published under the terms of the creative commons attribution licence 4.0

https://creativecommons.org/licenses/by/4.0/deed.en_US